

Supplementary Information (SI) accompanying

Pericytes and shear stress each alter the shape of a self-assembled vascular network

*Kazuya Fujimoto^a, Scott Erickson^a, Masamune Nakayama^a, Hiroki Ihara^a, Kei Sugihara^b,
Yuji Nashimoto^{†a}, Koichi Nishiyama^{‡c}, Takashi Miura^b, and Ryuji Yokokawa^{*a}*

^aDepartment of Micro Engineering, Kyoto University, Kyoto, Japan.

^bGraduate School of Medical Sciences, Kyushu University, Fukuoka, Japan.

^cInternational Research Center for Medical Sciences (IRCMS), Kumamoto University, Kumamoto, Japan.

*Ryuji Yokokawa

Department of Micro Engineering,

Kyoto University

Kyoto Daigaku-Katsura Nishikyo-ku

Kyoto 615-8540, Japan

Tel/Fax: +81-75-383-3680

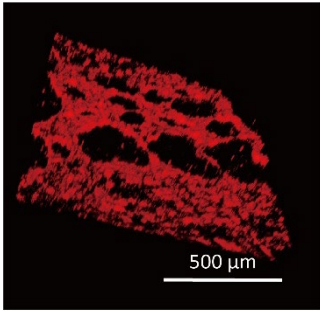
Email: yokokawa.ryuji.8c@kyoto-u.ac.jp

[†]Current affiliation: Institute of Biomaterials and Bioengineering, Tokyo Medical and Dental University, Tokyo, Japan.

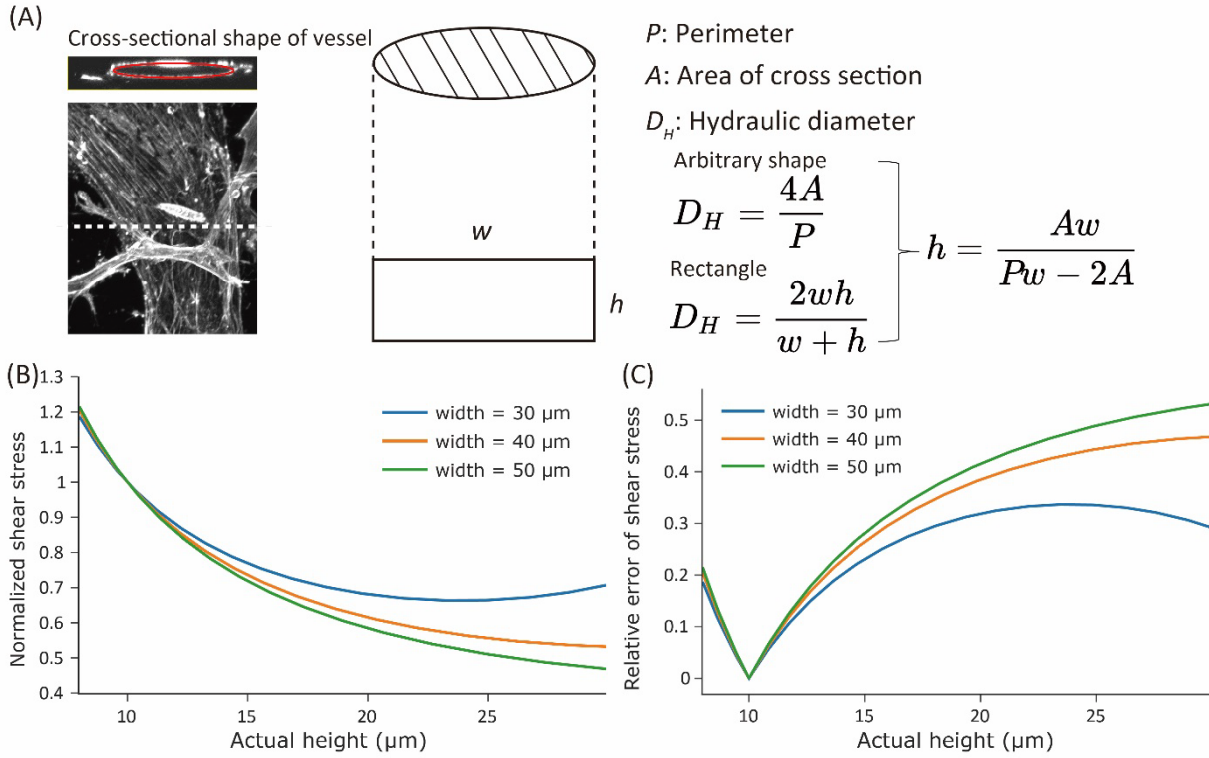
[‡]Current affiliation: Department of Medical Sciences, University of Miyazaki, Miyazaki, Japan.

Contents

1. Supplementary figure S1: 3D reconstruction of a self-assembled vascular network.
2. Supplementary figure S2: Error of shear stress caused by the difference in vessel height.
3. Supplementary figure S3: Contour plot of flow velocity and pressure by numerical simulation.
4. Supplementary figure S4: Immunostaining for platelet-derived growth factor (PDGF) and its receptor.
5. Supplementary figure S5: Time-lapse images for the pericyte migration in short-term.
6. Supplementary figure S6: Vessel diameter with pericytes in the presence of PDGF inhibitors.
7. Supplementary figure S7: Normalized vessel diameter without pericytes in the presence of PDGF inhibitor.
8. Supporting texts: Vessel height and shear stress error.
9. Supporting table 1: Statistical analysis results of flow rate effects on morphological parameters.

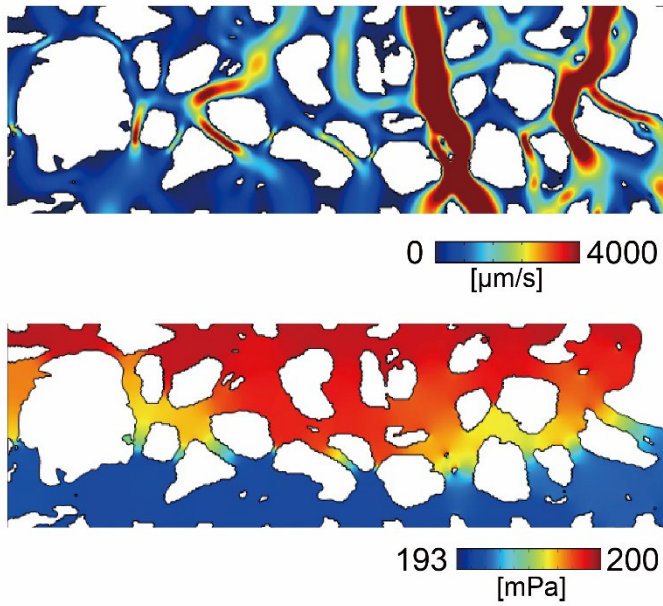


Supplementary figure S1: 3D reconstruction of a self-assembled vascular network. Vasculature formed by RFP-HUVECs in a microfluidic device was scanned using a laser scanning confocal microscopy and three-dimensionally reconstructed.



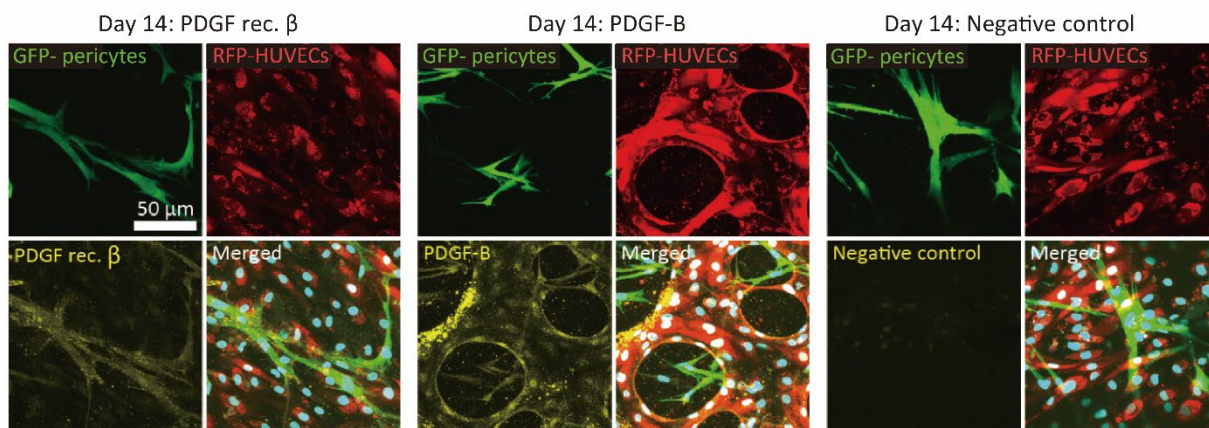
Supplementary figure S2: Error of shear stress caused by the difference in vessel height. (A)

Calculation of an equivalent height and width of a rectangle which gives identical hydraulic diameter calculated with A : area, P : perimeter, and w : width of the vessel measured from the cross-sectional shape of the vessel to consider the condition in the COMSOL simulation (Fig. 2E). (B) Normalized shear stress was calculated assuming the cross-sectional shape as a rectangle with 8~25 μm of height when the original vessel height in the x-axis was 10 μm . Shear stress is normalized by the value calculated with a vessel height of 10 μm , which is the setting used in the COMSOL simulation. The stresses were analytically calculated with three widths (30, 40, and 50 μm , SI text). (C) Relative error of shear stress calculated with the same setting (ESI text).

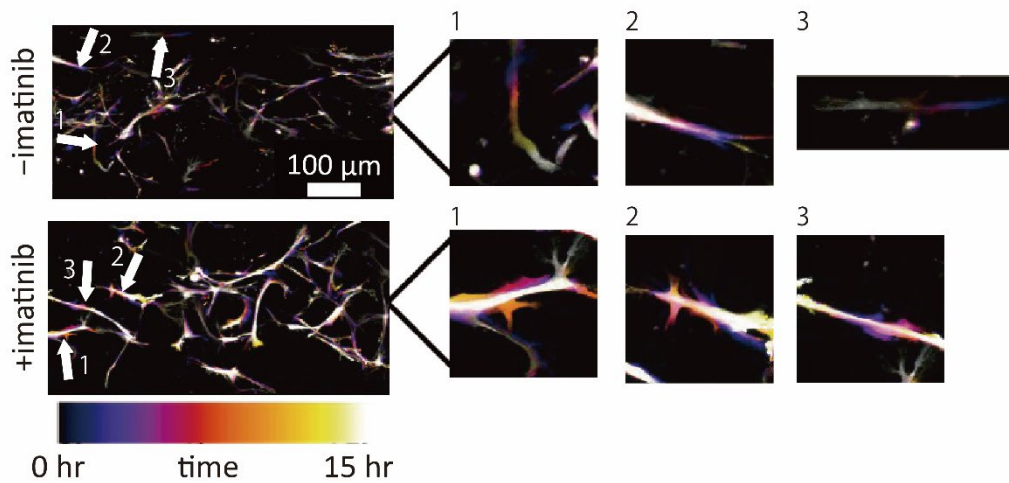


Supplementary figure S3: Contour plot of flow velocity and pressure by Numerical simulation.

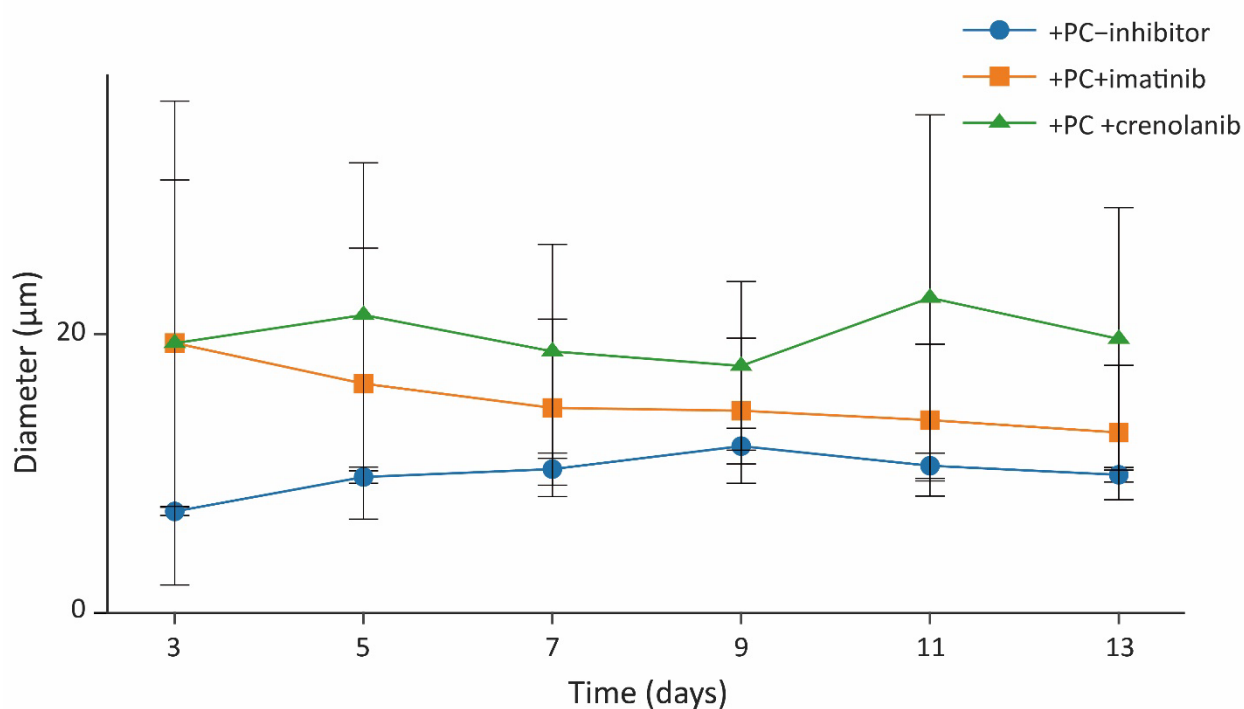
Flow velocity (top) and pressure (bottom) were calculated using vessels with an assumed height of 10 μm in COMSOL.



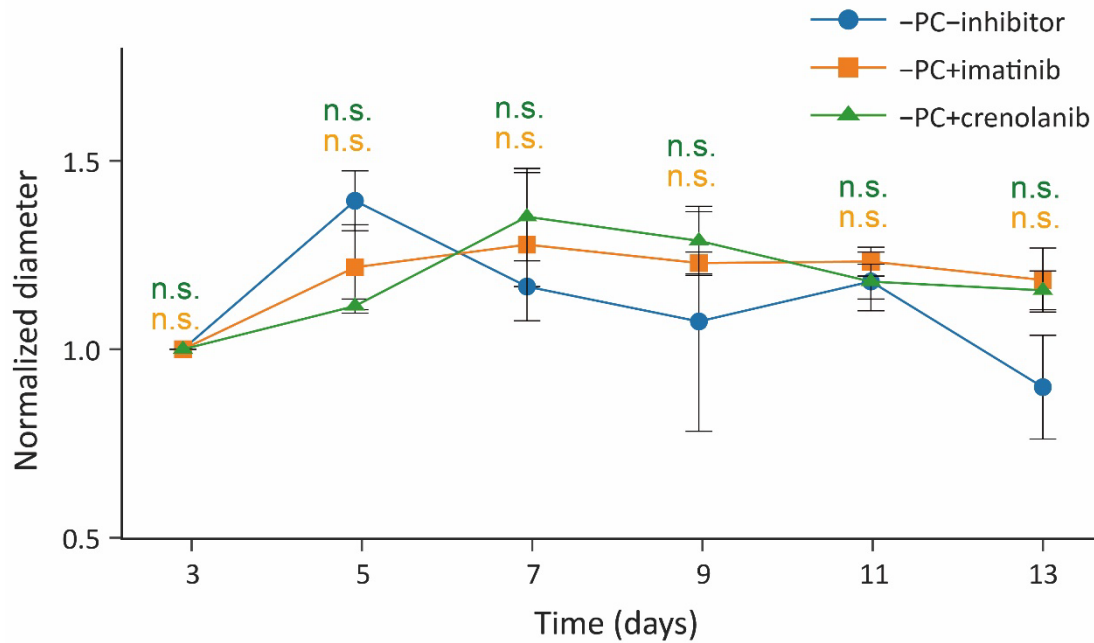
Supplementary figure S4: Immunostaining for platelet-derived growth factor (PDGF) and its receptor. Fluorescence images show expression of PDGF receptor β in GFP-pericytes and PDGF-B in RFP-HUVECs. The cells were stained on day 14 of the culture.



Supplementary figure S5: Time-lapse images for the pericyte migration in short-term. Images of pericytes in devices were captured every 30 min for 15 hours. Imaging started on day 12. Each frame was assigned a color (see color scale bar) and superimposed. Arrows indicate the extracted cells of interest to the right. Directed pericyte migration was observed more frequently in devices without imatinib, whereas random pericyte migration was observed more frequently in those with imatinib.



Supplementary figure S6: Vessel diameter with pericytes in the presence of PDGF inhibitors. These original diameters were used to calculate the normalized diameters plotted in Fig. 5D. Data represent the mean \pm standard deviation (S.D.) of at least three replicates of devices.



Supplementary figure S7: Normalized vessel diameter without pericytes in the presence of PDGF inhibitor. Vessel diameter was measured and normalized by the diameter on day 3. Crenolanib and imatinib do not have significant influence on the diameter. Diameter values are measured from the devices, and the average diameter is calculated. Data represent the mean \pm standard deviation (S.D.) of at least three replicates of devices. Statistical significance of the difference between -PC-inhibitor and -PC+imatinib, and between -PC-inhibitor and -PC+crenolanib were calculated for each time point. n.s., $p>0.05$.

Supporting texts: Vessel height and shear stress error.

We estimated the relationship between the error in vessel height and the relative error of shear stress in the numerical simulation. The velocity field for the Poiseuille flow in a rectangle is described as

$$v_x = \frac{4h^2 \Delta p}{\pi^3 \eta L} \sum_{n,odd}^{\infty} \frac{1}{n^3} \left[1 - \frac{\cosh\left(n\pi \frac{y}{h}\right)}{\cosh\left(n\pi \frac{w}{2h}\right)} \right] \sin\left(n\pi \frac{h}{z}\right)$$

Here, we will discuss shear stress along the center line at the middle of channel height ($z = h/2$). Shear stress along the line is as follows,

$$\begin{aligned} \tau_x(y, h/2) &= \frac{\partial v_x}{\partial y} \\ &= \frac{4h^2 \Delta p}{\pi^3 \eta L} \sum_{n,odd}^{\infty} \frac{1}{n^3} \left(-\frac{n\pi \sinh \frac{n\pi y}{h}}{\cosh \frac{n\pi w}{2h}} \right) (-1)^{n/2} \end{aligned}$$

To consider shear stress at the vessel wall, we substitute $y = -w/2$ and derive

$$\begin{aligned} &= \frac{4h^2 \Delta p}{\pi^3 \eta L} \sum_{n,odd}^{\infty} \frac{1}{n^3} \left(\frac{n\pi \sinh \frac{n\pi w}{2h}}{\cosh \frac{n\pi w}{2h}} \right) (-1)^{n/2} \\ &= \frac{4h^2 \Delta p}{\pi^3 \eta L} \sum_{n,odd}^{\infty} \frac{1}{n^3} \left(\frac{n\pi \tanh \frac{n\pi w}{2h}}{h} \right) (-1)^{n/2} \end{aligned}$$

The mass flow rate along the cross-section is constant since the flow rate of the syringe pump in the experiment was fixed. With the assumed height h and true height h' , the relationship of mass flow with h and h' derives as,

$$1 - 0.630 \frac{h'}{w} \Delta p' = 1 - 0.630 \frac{h}{w} \Delta p.$$

Here we defined the normalized shear stress as

$$\begin{aligned} \tau_{norm} &= \frac{\tau'_x}{\tau_x}, \\ &= \frac{\Delta p'}{\Delta p} \sum_{n,odd}^{\infty} \frac{h \tanh \frac{n\pi w}{2h'}}{h' \tanh \frac{n\pi w}{2h}} \\ &= \frac{1 - 0.630 \frac{h}{w}}{1 - 0.630 \frac{h'}{w}} \sum_{n,odd}^{\infty} \frac{h \tanh \frac{n\pi w}{2h'}}{h' \tanh \frac{n\pi w}{2h}} \end{aligned}$$

Relative shear stress error is calculated as

$$e_{rel} = \left| 1 - \frac{\tau'_x}{\tau_x} \right|.$$

We estimate the relative error by substituting $w = 30 \sim 50 \mu\text{m}$, $h = 10 \mu\text{m}$, $h' = 10 \sim 25 \mu\text{m}$ regarding measured height variance and plot them in Fig. S2.

Table 1 Statistical analysis results of flow rate effects on morphological parameters.

One-way ANOVA p-values					
Time (hours)	0	6	12	18	24
Normalized branches	0.343	0.0754	0.0436	0.00147	4.92E-05
Normalized junctions	0.343	0.0884	0.119	0.00152	0.000854
Normalized endpoints	0.343	0.0534	0.0206	3.56E-05	1.05E-05
Dunnett's test p-values					
Normalized branches	Time (hours)				
	Flow rate ($\mu\text{L/h}$)	6	12	18	24
	10	-	1.00	0.998	1.00
	30	-	0.370	0.0224	0.00198
	60	-	0.197	0.0083	0.00942
	120	-	0.314	0.0111	0.00016
Normalized junctions	Time (hours)				
	Flow rate ($\mu\text{L/h}$)	6	12	18	24
	10	-	-	0.999	1.00
	30	-	-	0.0738	0.0043
	60	-	-	0.0390	0.0550
	120	-	-	0.0172	0.0015
Normalized endpoints	Time (hours)				
	Flow rate ($\mu\text{L/h}$)	6	12	18	24
	10	-	1.00	0.990	0.993
	30	-	0.597	0.116	0.0392
	60	-	0.108	0.00016	4.50E-05
	120	-	0.224	0.00075	0.00023
			p < 0.05	p < 0.005	p < 0.0005